Correlative super-resolution fluorescence and metal replica transmission electron microscopy

Kem A. Sochacki[1,*], **Gleb Shtengel**[2,*], **Schuyler B. van Engelenburg**[3], **Harald F. Hess**[2,‡], and **Justin W. Taraska**[1,‡]

[1]National Heart Lung and Blood Institute, National Institutes of Health, Bethesda, Maryland 20892, USA

[2]Howard Hughes Medical Institute, Janelia Farm Research Campus, Ashburn, VA 20147, USA

[3]National Institute of Child Health and Human Development, National Institutes of Health, Bethesda, Maryland 20892, USA

Abstract

Super-resolution localization microscopy is combined with a complementary imaging technique, transmission electron microscopy of metal replicas, to locate proteins on the landscape of the cellular plasma membrane at the nanoscale. Robust correlation on the scale of 20 nm is validated by imaging endogenous clathrin (with 2D and 3D PALM/TEM) and the method is further used to find the previously unknown 3D position of epsin on clathrin coated structures.

Super-resolution localization microscopy (e.g. photoactivated localization microscopy, PALM[1]; or direct stochastic optical reconstruction microscopy, dSTORM[2]) can locate fluorescently labeled biomolecules at a resolution of 10–20 nanometers using multiple differently colored[3,4] or genetically encoded probes[1,3,5,6]. Interferometric PALM (iPALM)[6] adds an axial resolution of ~10 nm, best among 3D implementations. However, structure determination with localization microscopy is limited by labeling densities that do not satisfy the Nyquist sampling criterion. Furthermore, molecules that are not fluorescently labeled are invisible to fluorescent microscopy which results in images that lack their underlying cellular context. In contrast, platinum replicas viewed by transmission electron microscopy (TEM) provide 2 nm resolution images of the structural features of cells including the cytoskeleton, endo/exocytic vesicles, and all their associated protein complexes[7,8]. Identification of proteins in these images is usually done by ~15 nm immunogold labeling. Gold is, however, bulky which can cause sparse labeling, obscure the structural detail beneath, and is sometimes indistinguishable from dark EM areas. Thus, super-resolution localization microscopy and metal replica TEM are complementary

methods that can be combined to determine protein positions within a rich cellular context at the resolution of several nanometers in 2D or 3D.

Correlative super-resolution and EM is becoming an important control for verifying super-resolution data[1,9]. In these cases, empirical coarse overlays of images are sufficient. However, there is a lack of techniques that reproducibly correlate at the nanometer scale across large areas and are robust enough to allow statistical analysis of protein locations with previously unknown positions. Prior attempts have encountered three major difficulties: fluorescent probes that are incompatible with EM sample preparation, structural deformation between imaging modes, and a lack of alignment markers that are stationary at the nanoscale[5,10]. We have found that thin, coverslip-bound samples, like cell membranes, avoid these problems when grown on custom-designed gold nanoparticle embedded coverslips; this allows super-resolution 2D and 3D PALM imaging to be combined with metal replica TEM techniques[7,11]. With this combined technique we report reproducible nanoscale correlation across 20 μm images and statistical analysis of protein localizations on single clathrin-coated structures across the membrane.

Figure 1 shows the general imaging pipeline for fluorescent super-resolution microscopy - metal replica TEM. Importantly, cells were grown on coverslips containing gold nanorods embedded under a ~20 nm layer of silica. The silica covered nanorods have strong photoluminescence due to surface plasmon resonance and are visible in iPALM. They extended above the flat surface of the coverslip (Supp. Fig. S1) and transferred with the platinum replica which allowed them to be used as nanometer-scale iPALM-TEM correlation markers in the X-Y plane. Proteins were antibody labeled with Alexa Fluor 647 (AF647) and the membrane was labeled with myristoylated psCFP2, which allowed for iPALM/TEM alignment in the Z dimension.

First, we examined 2D correlation across entire cell membranes. A 2D TEM tiling of a membrane is shown in Fig. 2a. The X-Y PALM positions of AF647 antibody-labeled clathrin heavy chain (clathrin-AF647) are mapped onto the TEM images in Fig. 2b (and Supp. Fig. S2). This was done with a first degree polynomial spatial warp transformation that registers positions of gold nanoparticles in PALM and TEM data. For eight cells, 6 to 22 nanoparticles were used for each transformation (ave. = 16 nanoparticles) and the averaged registration error for nanoparticles in each cell ranged from 3.6 nm to 10.1 nm. X-Y localizations from clathrin-AF647 in the PALM image match the 2D shapes of the clathrin coated structures (CCSs) in TEM (Figs. 2c–d). AF647 is linked to clathrin through a 20–25 nm antibody complex and therefore the fluorescence of a structure is generally larger than that of the TEM image. To assess how the fluorescence mapped to the CCSs, we created average two-dimensional fluorescence density maps of clathrin-AF647 X-Y PALM localizations with respect to 2D TEM structures (Figs. 2e–f, see methods for details). CCSs were split into two categories based on how their three-dimensional geometries would be projected onto the X-Y plane. The first category, flat and slightly domed pits (short; Fig. 2e green), should roughly exhibit uniform fluorescence within the perimeter of the CCS (Fig. 2f purple). Highly domed pits (tall; Fig. 2e orange), however, should exhibit the profile of a hemispherical shell, with intensity peaking near the radius of the shell and dipping in the center (Fig. 2f blue). Fluorescence density maps (Figs. 2e) provide a picture of how well

clathrin-AF647 fluorescence correlated to the geometric clathrin lattice observable in TEM. Radial profiles of the average images are shown in Fig. 2e (bottom right). For short (green) and tall (orange) CCSs, the profiles agree with geometric simulations of flat (Fig. 2f, purple) and hemispherical (Fig. 2f, blue) objects of radius, r=50 nm, with 25 nm shells extending from their surfaces (accounting for the immuno-tether), and convolved with a Gaussian of σ=16 nm. We attribute this convolution factor (σ =16 nm) to a combination of errors including PALM/TEM registration, PALM localization, and visually defining the perimeters of CCSs in TEM. Even with these errors, the average fluorescence density maps demonstrate the close 2D correlation obtainable by this method.

After a two dimensional correlation had been performed, fluorescence was further correlated to 3D tomograms by matching features between the tomogram and the two-dimensional TEM image. Correlation in the axial dimension (Z) was attained by aligning the iPALM Z-position of a fluorescent membrane marker (myristoylated psCFP2) to the TEM membrane plane (Fig. 2g). Gold nanoparticles could not be used for the Z-dimension alignment because they shift in Z with respect to the rest of the replica during lifting. Four CCSs are shown in three dimensional correlations in Fig. 2h (more in Supp. Movies S1 and S2). The shapes of the pits in the Z-dimension in iPALM images match the shapes of the corresponding pits in the TEM tomograms. Occasionally, there were regions where the fluorescence membrane marker did not align with the TEM membrane (< 10% membrane area). These regions tended to be where there was a wide (~ 1 μm) non-adherent domed membrane patch visible in iPALM which likely collapsed during critical point drying or replica transfer to the TEM grid. In these cases, there was clear membrane misalignment (see Supp. Fig S3, Movie S3) and CCSs were not analyzed. Myristoylated psCFP2 was rarely found inside of clathrin structures but was often found in non-clathrin vesicles (Supp. Movie S3) suggesting that myristoylated proteins may be excluded. The clathrin-AF647 fluorescence along the Z dimension was assessed with one dimensional fluorescence histograms of 96 CCSs in Fig. 2i. Histograms were normalized and ordered by height (as measured from TEM). For the range of heights, clathrin fluorescence (magenta) extends from 20–30 nm above the plasma membrane (blue) to ~25 nm above the top of the clathrin structure observed by TEM (orange). These distances are consistent with fluorophores attached to a 25 nm antibody complex that coats the top of a dome. The small differences between fluorescence and TEM data in YZ results from errors discussed above as well as possible drying effects from the TEM preparation. We attribute the low registration error to the thin fixed sample adhered to the coverslip for both iPALM imaging and TEM preparation.

After validating our method with clathrin, we applied it to the endocytic protein, epsin 1. Epsin binds clathrin, the lipid phosphatidylinositol-4,5-bisphosphate, ubiquitinated cargo, eps15 homology domains, and the adapter complex AP2, and has been proposed to generate membrane curvature, facilitate vesicle scission, traffic ubiquitinated cargo, and regulate actin[8,12–16]. With such diverse functions in dispute, it is unclear how epsin functions in endocytosis. Epsin is highly colocalized with clathrin in live cells with diffraction-limited fluorescence (Supp. Fig. S4). Understanding the physical location of epsin within clathrin structures at the nanometer scale would help to unravel epsin's role in endocytosis. The position of AF647-labeled epsin 1 (epsin-AF647) at CCSs is shown in Fig. 3a and Supp.

Fig. S5. In two-dimensional correlative images for the CCSs (327) observed in three cells, epsin appeared at the outer perimeter of most structures (81%) including both flat structures and highly curved pits (Fig. 3a). There were, however, cases (18%) where epsin was distinctly found at the center. Less than 1% of CCSs had no detectable epsin-AF647. All CCSs from a single cell are displayed in Supp. Fig. S6. Because epsin-AF647 was often visible as less than five puncta per structure, averaging needed to be done to assess the two-dimensional probability density for 159 slightly domed (or flat; Fig. 3b) and 84 highly domed (Fig. 3c) structures as was previously done for clathrin. The average probability density map for epsin is compared to that of clathrin for short and tall structures in Fig. 3d. In both cases, the fluorescence from epsin-AF647 dips lower in the center and reaches its maximum further from the center than clathrin-AF647. This confirms the visual analysis that epsin is statistically concentrated at the perimeter of CCSs in the XY plane. Control experiments using two-color PALM (or dSTORM) imaging of clathrin-ATTO488 and epsin-AF647 in intact vs. unroofed cells demonstrate that our protein locations are not changed during our unroofing preparation or correlative imaging pipeline (Supp. Fig. S7). Epsin could also be labeled with photoconvertible fluorescent protein like mEos3 (Supp. Fig. S8), but the benefits of observing the native protein and the higher resolution obtained from the brighter AF647 were superior for statistical analysis. Tomograms for six CCSs are shown in Supp. Movies S4 and S5 and the position of epsin-AF647 in the Z-dimension was analyzed (as done for clathrin) in Fig. 3e. Strikingly, the position of epsin-AF647with respect to CCSs in the Z-dimension looks similar to clathrin-AF647. This indicates that epsin is not located exclusively at the base of CCSs but instead samples the entire height of the CCSs during all stages of endocytosis. To illustrate this, we created 3D isosurface models of TEM tomograms and epsin-AF647 iPALM renderings (Fig. 3f–h and Supp. Movie S6). These models show that while the fluorescence is at the outer perimeter of CCSs in the X-Y plane, it appears anywhere along the height of clathrin pits.

Our data provides a map of proteins at single endocytic structures and helps form models of these proteins' functions. For example, epsin has been suggested to induce curvature of CCSs[12,15]. We show that epsin 1 is not concentrated in regions of specific curvature. Instead, epsin is enriched and depleted in regions of equivalent curvature (edge and center of flat CCSs, or side and top of clathrin pits). Our data also shows that epsin is not part of the complex that is located at the bottom rim of CCSs which has been previously suggested[13,16]. Our data suggest that interaction with the rim complex is either transient or not specific. A complete map of all the molecules associated with these structures is possible with this method and will provide a comprehensive structural view of endocytosis in cells.

Materials and Methods

Coverslips

Gold nanorods (25×45 nm, part # A12-25-650, Nanopartz, Colorado) were deposited on the surface of poly-L-lysine (Sigma) coated 25 mm round coverslips of #1.5 thickness (Warner Instruments, Hamden, Connecticut). SiO_2 (~20 nm thick) was sputtered over top of the nanorods using a Denton Explorer sputtering system (Denton Vacuum, Moorestown, New

Jersey). These coverslips were cleaned and coated with poly-L-lysine prior to plating the cells.

Cell Culture and Transfection

PC12-GR5 cells were maintained at 37°C and 5% CO2 in T75 flasks (Sarsdtedt 83-1813-002) in dye-free DMEM (Life Technologies 21063-029) supplemented with 5% fetal bovine serum and 5% horse serum. Transfections were performed with Lipofectamine 2000 (Invitrogen) and 2 μg of plasmid after one day of growth on coverslips. The myristoylated psCFP2 expression constructed was made by PCR amplification of the psCFP2 gene (Evrogen) including the mammalian codon optimized myristoylation signal peptide from the v-src gene: MGSSKSKPKDPSQRRNNN. The amplicon was subsequently cloned into the empty N1 mammalian expression vector (Clontech) using the BglII (5′) and NotI (3′) restriction sites. pEGFPC1-Epsin1 was obtained from Addgene (#22228). Epsin1-mcherryC1 and Epsin1-mEos3 were both made by replacing EGFP from pEGFPC1-Epsin1 with mCherry (Clontech #632524) or mEos3[19] using Age1 and BsrG1. For live imaging, cells were transfected with 1 μg each of pEGFP-LCa (clathrin light chain a)[20] and pmCherryC1-Epsin1.

Unroofing

One day after transfection, cells were rinsed with imaging buffer (130 mM NaCl, 2.8 mM KCl, 5 mM $CaCl_2$, 1 mM $MgCl_2$, 10 mM Hepes, 10 mM glucose, pH 7.4), briefly incubated in one part stabilization buffer (70 mM KCl, 30 mM HEPES at pH 7.4, 5 mM $MgCl_2$, and 1 mM DTT) and three parts 0.01% w/v poly-lysine for 10–15 sec, and then incubated for 10–15 seconds 3 times in a fresh solution made of one part stabilization buffer and three parts water. The coverslips were then placed in stabilization buffer containing fixative (2% paraformaldehyde and 0.04% glutaraldehyde, Electron Microscopy Sciences) immediately before sonication. Sonication was done with a Branson Sonifier 450 with a 1/8″ tapered microtip. The tip was positioned 5 mm above the coverslip and a single 400 ms pulse at the lowest output setting resulted in approximately 1 cm^2 of unroofed cells on the coverslip. The cells were then placed into fresh stabilization buffer and fixed for 20 min.

Immunolabeling

Fixed unroofed cells were rinsed with PBS and placed into blocking buffer (PBS with 3 % w/v bovine serum albumin, BSA) for one hour. The unroofed cells were then incubated for one hour in blocking buffer containing 2 μg/mL primary antibody (R-20, Santa Cruz Biotechnology or X22, ThermoScientific). The sample was rinsed with blocking buffer prior to secondary antibody labeling for 30 min (2 μg/mL Alexa Fluor 647 donkey anti-goat, Invitrogen A31571; Alexa Fluor donkey anti-mouse, Invitrogen A21447; or Atto 488 donkey anti-mouse) in blocking buffer. Atto 488 donkey anti-mouse was created with Atto 488 NHS ester (Sigma, 4-molar excess) and unlabeled donkey anti-mouse IgG (Abcam ab6707) and purified through a Superdex 75 10/300 GL size exclusion column (GE Healthcare). Finally, the sample was washed with blocking buffer, PBS, and post-fixed for 20 min. For immunolabeling intact cells, 0.2% Triton X was added to the blocking buffer, and cells were incubated for two minutes in permeabilization buffer (PBS 3 % w/v BSA, 0.5% Triton X) prior to blocking.

iPALM

After immunolabeling, cells were rinsed, placed in blinking buffer (50 mM Tris, 10 mM NaCl, 0.1 g/mL glucose, 0.8 mg/mL glucose oxidase, 40 μg/mL catalase, 71 mM 2-mercaptoethanol), and covered with a 18 mm #1.5 coverslip. The two coverslips were sealed with epoxy (Elmer's products, Inc, Columbus, Ohio) and Vaseline (Unilever, Greenwich, Connecticut). iPALM was performed as previously described[6] with the z-axis measurement range extended to 750 nm[3]. Typical iPALM data acquisition consisted of 40,000–80,000 frames acquired with iXon DU-897E EM-CCD cameras (Andor, UK). Acquisition was performed in frame transfer mode and the laser excitation was constantly active during acquisition. AF647 was imaged with a 637 nm MRL-III-640 laser (OptoEngine, Midvale, UT) at ~3000 W/cm^2 with 20–30 ms exposure using LP02-647RU and FF01-720/SP filters. psCFP2 was imaged with 488 nm Cyan 488 laser excitation (Newport, Spectra Physics, Santa Clara, CA) at ~400 W/cm^2 with 50 ms exposure using LP02-488RS and FF01-520/35 filters. An additional quad notch filter NF01-405/488/561/635 was used for all imaging. Filters were from Semrock (Rochester, NY).

The iPALM calibration procedure and data analysis have been previously described[3,6,21]. Two-channel iPALM image registration was performed using Au nanoparticles. The same nanoparticles were observed under 647 nm illumination and 488 nm illumination which allowed for registration of two channels[3]. Images of iPALM data were rendered as previously described[1,6].

After iPALM imaging of several areas (each containing 1–3 unroofed cells), a 3 mm circle was etched into the coverslip around the area with a diamond objective marker (#11505059, Leica Microsystems, Buffalo Grove, IL). The entire area was imaged with 10x differential interference contrast (DIC). The image was used as a map to locate cells in TEM. The coverslip sandwich was separated and the sample was placed in HBSS (Hank's balances salt solution, Life Technologies) containing 2% glutaraldehyde at 4 °C overnight.

Electron Microscopy

Samples were critical-point-dried and coated with platinum and carbon as previously described[22]. The coated samples were imaged with 10x phase contrast light microscopy to locate the regions of interest (ROIs). A pioloform and carbon coated 50-mesh, 3 mm copper grid was plasma discharged and dipped in a 1:5 dilution of goat anti-mouse 10 nm immunogold conjugate (EM.GMTA10, BBinternational, Cardiff, UK) rinsed and dried on filter paper. This resulted in sparsely scattered gold nanoparticles that were used as fiducials for tomogram alignment.

The platinum-carbon replica was lifted off of the coverslip by floating the sample on 5% hydrofluoric acid. The replicas were rinsed using successive dilutions with water, lifted out of the water and placed onto the grid using a Perfect Loop (Electron Microscopy Sciences). The replica was again imaged with 10x phase contrast light microscopy to find the placement of the ROIs with respect to the grid. In some cases, there was loss of a ROI because it was placed over a grid bar.

Transmission electron microscopy was performed on a JEOL 1400 running SerialEM freeware[17] and equipped with a XR-111 CCD camera (AMT, Wobum, MA) Montages of entire unroofed cells were produced at 15000x with 10% overlap. Single axis tilt series (−60° to 60°, 1° increments) were collected at 8000x. The montages were stitched together and the tilt series were reconstructed into tomograms using IMOD software[17,18].

Correlation

The 25×45 nm gold nanorods were identified in TEM micrographs. The procedure used for two-color PALM alignment[3] was also used to register 2-color PALM images to the TEM images. For image correlations we used a POLYWARP1 image transformation defined as:

$$X^{'}=K_{x00}+K_{x01} \cdot X+K_{x10} \cdot Y+K_{x11} \cdot X \cdot Y$$
$$Y^{'}=K_{y00}+K_{y01} \cdot X+K_{y10} \cdot Y+K_{y11} \cdot X \cdot Y$$

where X and Y are the PALM gold coordinates being transformed to the TEM gold coordinates, $X^{'}$ and $Y^{'}$. K coefficients were calculated with a least-squared solution.

After X-Y PALM data was aligned to the 2D TEM data, the 10 nm gold nanospheres were used as markers to align the 2D TEM/iPALM correlation to the 3D tomogram (in the XY plane) using linear regression or POLYWARP1. Z-alignment was performed by manually aligning the membrane iPALM marker with the membrane in TEM tomograms across the entire tomogram.

Fluorescence probability density maps

Two-dimensional EM micrographs were analyzed in ImageJ[23] and elliptical regions of r_x and r_y (radii along the X and Y axes) were drawn to best fit the shape of visible clathrin lattices. Clathrin structures were split into two categories: flat or slightly curved domes, and highly invaginated pits. Clathrin structures were omitted from this analysis only if they were at the edge of the cell, did not fit well to an ellipse, within 0.5 μm of a gold nanorod, or right next to another clathrin structure. In Matlab (Mathworks), the coordinates of PALM localizations were mapped onto the coordinates of the ellipses and assigned a fractional position from $-2r_x$ to $2r_x$ in the X dimension and $-2r_y$ to $2r_y$ in the Y dimension. The fractional coordinates from each ellipse were binned into a 40×40 two-dimensional histogram. The resulting image was normalized prior to averaging the images from all regions of a specific category (Figs. 2e,f and 3b,c). Radial scans were produced by averaging pixels based on their distance away from the center of the image. The standard error of pixel sampling takes into account the total number of pixels included in the final data point (from each separate 2D histogram).

Z-axis histograms

The height of each structure was determined by selecting the local plasma membrane plane and the top of the clathrin structure in TEM tomograms. A one-dimensional histogram of the Z-position of all iPALM localizations associated with each structure was mapped with

respect to the TEM coordinates. Finally, histograms were aligned by their bottom TEM coordinate (the plasma membrane) and arranged in order of height to create Figs. 2j and 3e.

Two-color localization microscopy (for Fig. S7)

Unroofed cells were prepared as for correlative microscopy. Intact cells were rinsed with imaging buffer and fixed with 2% paraformaldehyde. Immunolabeling clathrin heavy chain with Atto 488 and epsin 1 with AF647 is described above. Fixed and immunolabeled cells were placed in blinking buffer and imaged with a Nikon N-STORM super-resolution microscope system (N-1245) equipped with a CFI SR Apochromat TIRF 100x oil objective, a 80mW 488nm laser, a 125 mW 647 nm laser, and an Andor Ixon Ultra DU-897 camera. Two-color images were acquired in TIRF at full laser power with 20 ms frames. Final super-resolution images were localizations from 20–30,000 frames (each color).

AFM

Tapping-mode AFM images of clean coverslips were obtained in air with a multimode atomic force microscope driven by a NanoScope V controller and E scanner (Veeco/Bruker, Santa Barbara, CA), using AC160TS cantilevers (Olympus, Tokyo, Japan) with a typical resonance frequency of 300 kHz and a nominal spring constant of 42 N/m. Images were analyzed using NanoScope software (version 7).

Live TIRF

Cells were grown on poly-L-lysine coated 25 mm round coverslips of #1.5 thickness (Warner Instruments, Hamden, Connecticut) and transfected with pEGFP-LCa (clathrin light chain a)[20] and pmCherryC1-Epsin1. Cells were imaged by total internal reflection fluorescence (TIRF) in imaging buffer as described previously[22]. Each image shown is an average of five subsequent 100 ms frames each 500 ms apart.

Supplementary Material

Refer to Web version on PubMed Central for supplementary material.

Acknowledgments

References

1. Betzig E, et al. Science. 2006; 313:1642–1645. [PubMed: 16902090]

2. Heilemann M, et al. Angewandte Chemie International Edition. 2008; 47:6172–6176.

3. Brown TA, et al. Molecular and cellular biology. 2011; 31:4994–5010. [PubMed: 22006021]

4. Bates M, Huang B, Dempsey GT, Zhuang X. Science. 2007; 317:1749–1753. [PubMed: 17702910]

5. Kopek BG, Shtengel G, Grimm JB, Clayton DA, Hess HF. PLOS ONE. 2013; 8:e77209. [PubMed: 24204771]

6. Shtengel G, et al. Proceedings of the National Academy of Sciences. 2009; 106:3125–3130.

7. Collins A, Warrington A, Taylor KA, Svitkina T. Current Biology. 2011; 21:1167–1175. [PubMed: 21723126]

8. Engqvist-Goldstein ÅE, et al. The Journal of cell biology. 2001; 154:1209–1224. [PubMed: 11564758]

9. Suleiman H, et al. eLife. 2013; 2

10. Watanabe S, et al. nature methods. 2010; 8:80–84. [PubMed: 21102453]

11. Heuser J. The Journal of cell biology. 1980; 84:560–583. [PubMed: 6987244]

12. Ford MG, et al. Nature. 2002; 419:361–366. [PubMed: 12353027]

13. Boucrot E, et al. Cell. 2012; 149:124–136. [PubMed: 22464325]

14. Hawryluk MJ, et al. Traffic. 2006; 7:262–281. [PubMed: 16497222]

15. Horvath CA, Vanden Broeck D, Boulet GA, Bogers J, De Wolf MJ. The international journal of biochemistry & cell biology. 2007; 39:1765–1770. [PubMed: 17276129]

16. Saffarian S, Cocucci E, Kirchhausen T. PLoS biology. 2009; 7:e1000191. [PubMed: 19809571]

17. Mastronarde DN. Journal of structural biology. 2005; 152:36–51. [PubMed: 16182563]

18. Kremer JR, Mastronarde DN, McIntosh JR. Journal of structural biology. 1996; 116:71–76. [PubMed: 8742726]

19. Zhang M, et al. nature methods. 2012; 9:727–729. [PubMed: 22581370]

20. Gaidarov I, Santini F, Warren RA, Keen JH. Nature cell biology. 1999; 1:1–7. [PubMed: 10559856]

21. Kanchanawong P, et al. Nature. 2010; 468:580–584. [PubMed: 21107430]

22. Sochacki KA, et al. Nature communications. 2012; 3:1154.

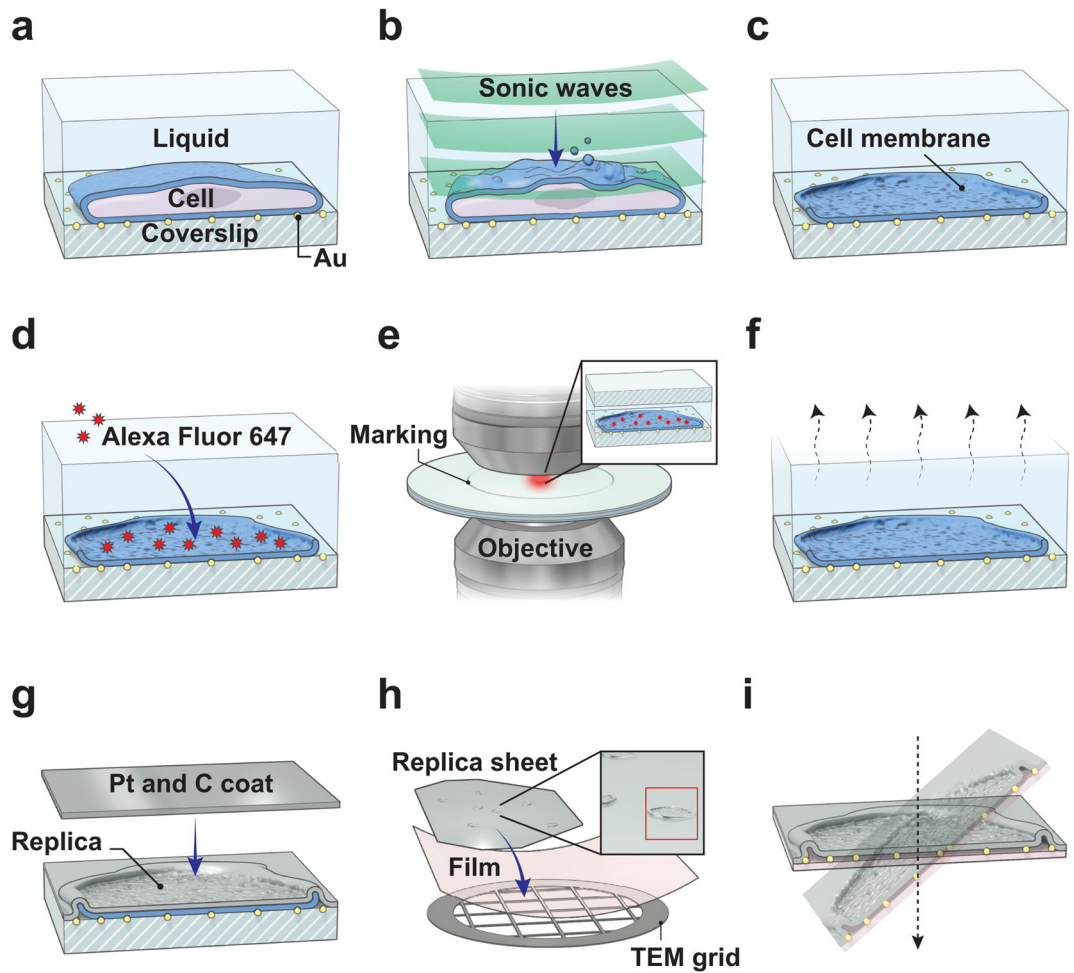23. Schneider CA, Rasband WS, Eliceiri KW. Nat Methods. 2012; 9:671–675. [PubMed: 22930834]

Figure 1. iPALM and TEM correlation imaging pipeline

a, PC12 cells were grown and transfected (for myristoylated psCFP2 membrane label) on a coverslip embedded with gold nanorods. The gold nanorods on these coverslips were covered in a ~20 nm layer of silica (Supp. Fig. S1). **b–c,** Cells were fixed and sonication was used to disrupt the upper cell membrane and expose the inner surface of the plasma membrane (unroofing). **d–e,** The protein of interest was immuno-labeled with Alexa Fluor 647. This and membrane-bound psCFP2 were imaged with iPALM. An objective style diamond scriber was used to mark a circle around the area that was imaged and a low magnification DIC image was acquired to create an atlas of the region. **f–g,** The sample was dehydrated and dried using a critical point dryer and coated with a thin layer of platinum and carbon to create a replica of the membrane surface. **h,** The replica was separated from the coverslip with 5% hydrofluoric acid, rinsed with successive water dilutions, and then transferred to a TEM grid. The glass-embedded gold nanorods visible in iPALM adhered to and were transferred with the platinum replica. **i,** The same cells that were imaged in iPALM were imaged with two-dimensional tiling in TEM with 15000x magnification. Sub-regions of these cells were imaged with 8000x magnification at 120 angles which were used to create three-dimensional tomograms[17].
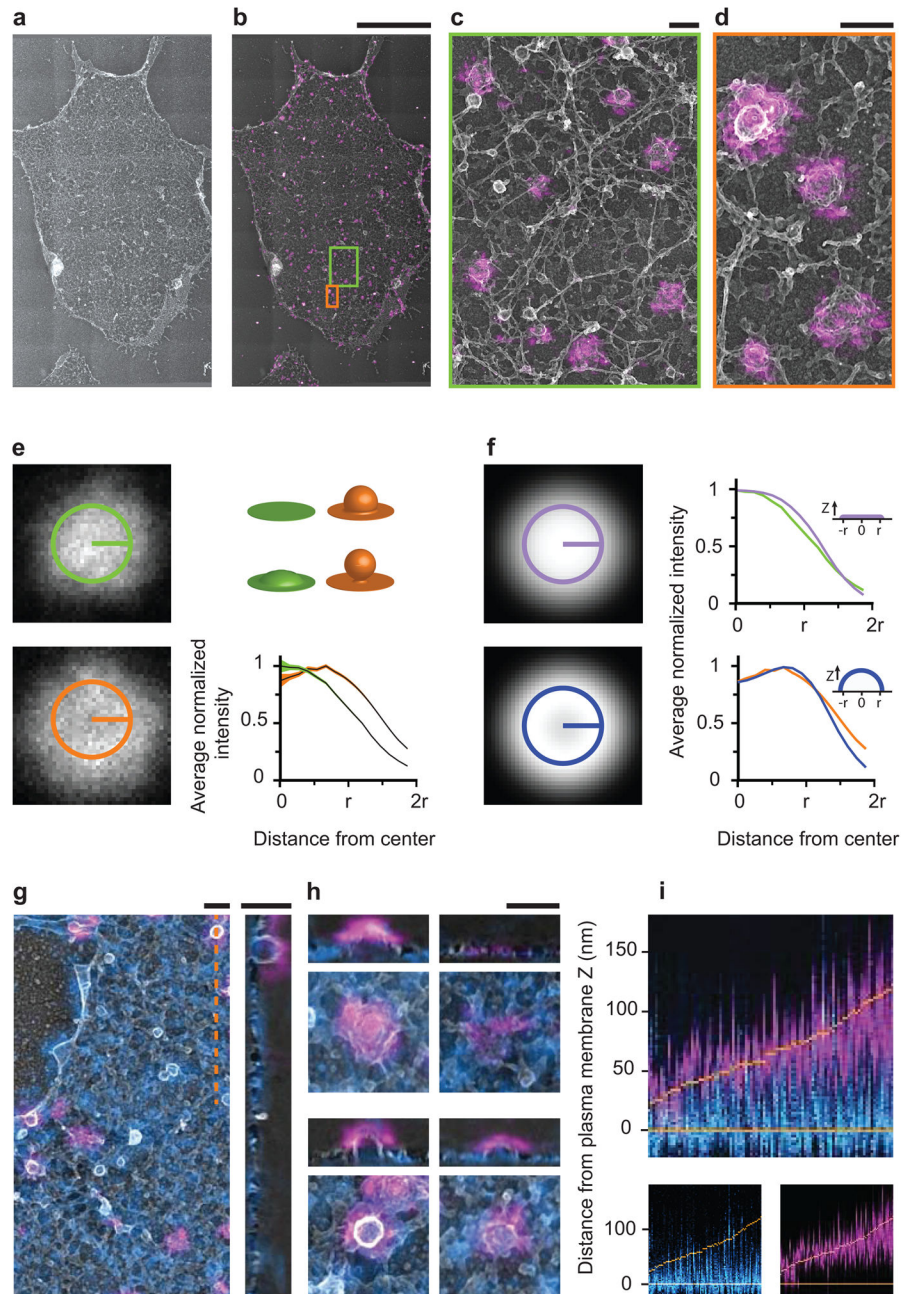
Figure 2. Correlation of clathrin fluorescence and clathrin TEM structures
a, Two dimensional TEM tiling of an unroofed cell replica. **b,** iPALM image of AF647 labeled clathrin heavy chain mapped onto the TEM image. Scale Bar 5 μm. **c–d,** Higher magnification images of b. Scale bars 200 nm. **e,** Average two-dimensional fluorescence density maps of 154 flat or slightly domed clathrin structures (green) and 116 highly domed clathrin structures (orange). **f,** Geometric models of a flat disk (purple, top) or hemispherical shell (blue, bottom) for comparison with e. Both are modeled with the radius, $r = 50$ nm, a 25 nm shell extending from its surface simulating the 25 nm immuno-linker as shown, and convolved with a two-dimensional Gaussian of $\sigma = 16$ nm. Radial scans of the images

generated by these geometric models are shown at the right compared with the data from e. **g,** Myristoylated psCFP2 (blue) and clathrin-AF647 (magenta) fluorescence are shown mapped onto the Z-projection of a tomogram. A magnified Z-slice along the orange dashed line is also shown. Scale bars 200 nm. **h,** Individual clathrin structures are shown in XY (Z-projection) and YZ (tomogram slice). Scale bar 200 nm. **i,** One dimensional histograms of fluorescence positions of myristoylated psCFP2 (blue) and clathrin-AF647 (magenta) in the Z-dimension were produced from 96 separate CCSs (3 tomograms) and shown here ordered by height. The local membrane plane and the top of the corresponding CCSs as observed by TEM are marked in orange and each histogram is aligned to bring this local TEM membrane plane to zero. The membrane and clathrin data are separated below for clarity.
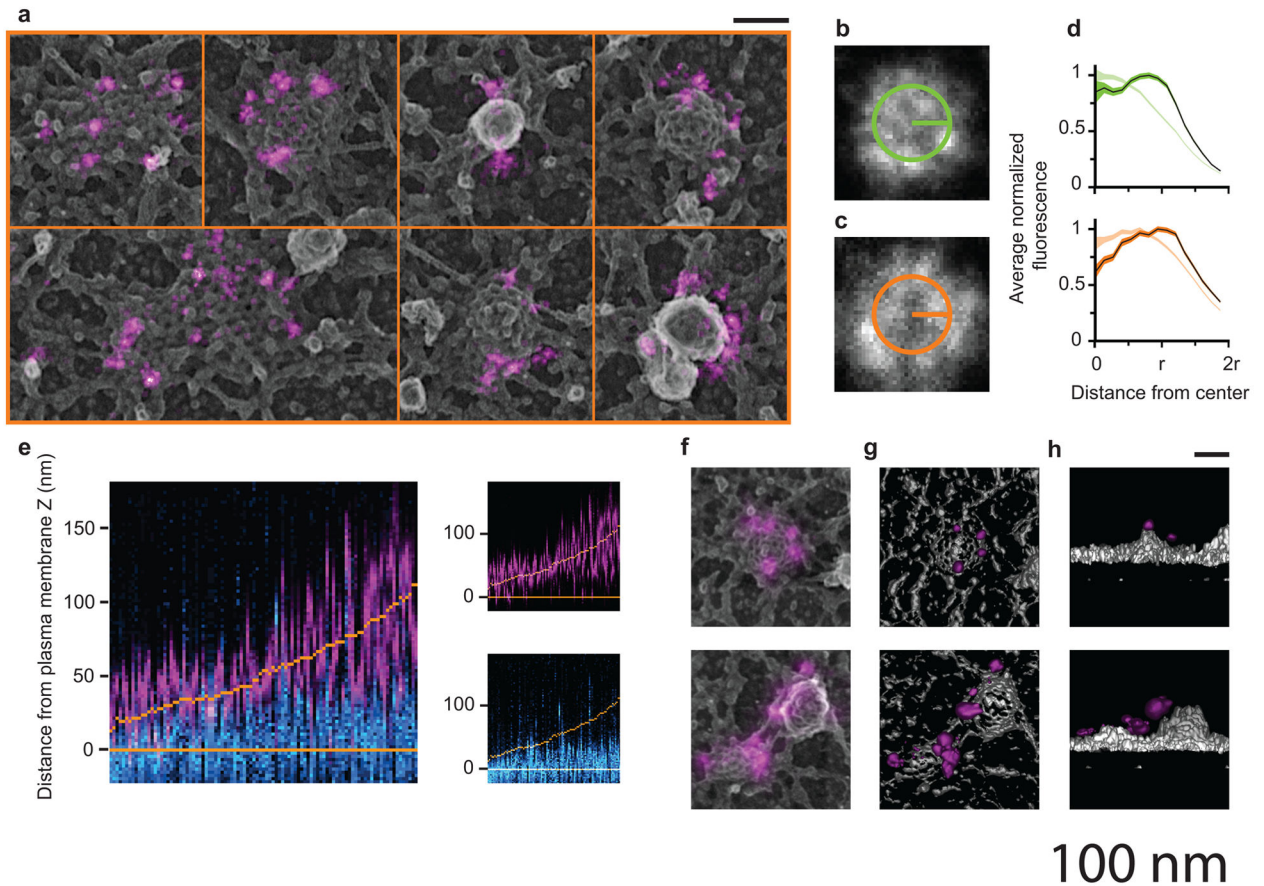
Figure 3. Epsin 1 is located around the outer perimeter in XY and along the entire height of the clathrin structure in Z

a, Epsin-AF647 fluorescence (magenta) correlated to TEM images (grayscale) in the XY dimension. The seven selected images all contain a clathrin structure in the center as evidenced by the geodesic mesh pattern. Scale bar 100 nm. **b–c,** Average fluorescence density maps of epsin for short (b; green) and tall (c; orange) clathrin structures as performed for clathrin heavy chain in Figs. 2e–f. **d,** Radial scans of the images in b (green opaque) and c (orange opaque) compared to their respective clathrin radial scans from Fig. 2g (lighter hue). The widths of the profiles depict the standard error of pixel sampling from each separate structure. **e,** 97 one-dimensional histograms of epsin-AF647 (magenta) and psCFP2 (cyan) fluorescence localizations along the Z-dimension placed in order of height. The plane of the plasma membrane and the top of the CCS as observed in TEM is shown in orange. All histograms were aligned to the position of the plasma membrane. **f,** Three CCSs with epsin-AF647 shown as Z-projections through the tomogram. **g,** Isosurface models (produced by imod freeware[18]) of the tomograms viewed down the Z-axis and, **h,** the Y-axis. Scale bar is 100 nm.